

73217**Impact Melt Breccia
St. 3,138.8 g****INTRODUCTION**

73217 is a tough impact melt; its bulk groundmass may be the low-K Fra Mauro basalt composition common at the Apollo 17 landing site but data is lacking. The rock contains a prominent white anorthosite clast (Fig. 1) as well as conspicuous and abundant fragments apparently derived from a plutonic gabbro with plagioclase, exsolved pyroxenes, and ilmenites. Brown silicic glass is conspicuous. Zircon clasts, probably part of the gabbro, have been dated as 4.36 Ga old. 73217 is medium gray (N5), subangular and blocky and has dimensions of 6.5 x 4.5 x 3.0 cm. The clast distribution is varied, with one face more rubbly with a

different lithology comprising 20% of the rock and consisting of clasts and matrix. Zap pits are irregularly distributed; the sample was collected from a half-buried position. Cavities and vesicles are uncommon except on the rubbly face. Allocations of 73217 have been made from chipped samples (e.g., Fig. 2).

PETROGRAPHY

Most published petrographic work has concentrated on the clasts and not on the general matrix of the breccia. Most of the thin sections consist of abundant mineral clasts in a fine-grained impact melt

groundmass (Fig. 3a). However, lithic clasts are present, particularly coarse granoblastic feldspathic impactites and the remains of a gabbro phase with feldspar, two pyroxenes (with complex exsolution) and ilmenite (Fig. 3b) with little host melt present. The rock and its clasts looks very similar to 73155.11e augitic pyroxenes contain numerous inclusions very similar to those in 73155. Many mineral clasts have thin rims formed post-brecciation by overgrowth or reaction. Silicic brown glass is conspicuous particularly where the gabbro exists. Its petrographic nature is uncertain; in places it appears to be relict mesostasis of the gabbro, but



Figure 1: Pre-processing photograph of sample 73217. Scale divisions in centimeters. S-73-16786.

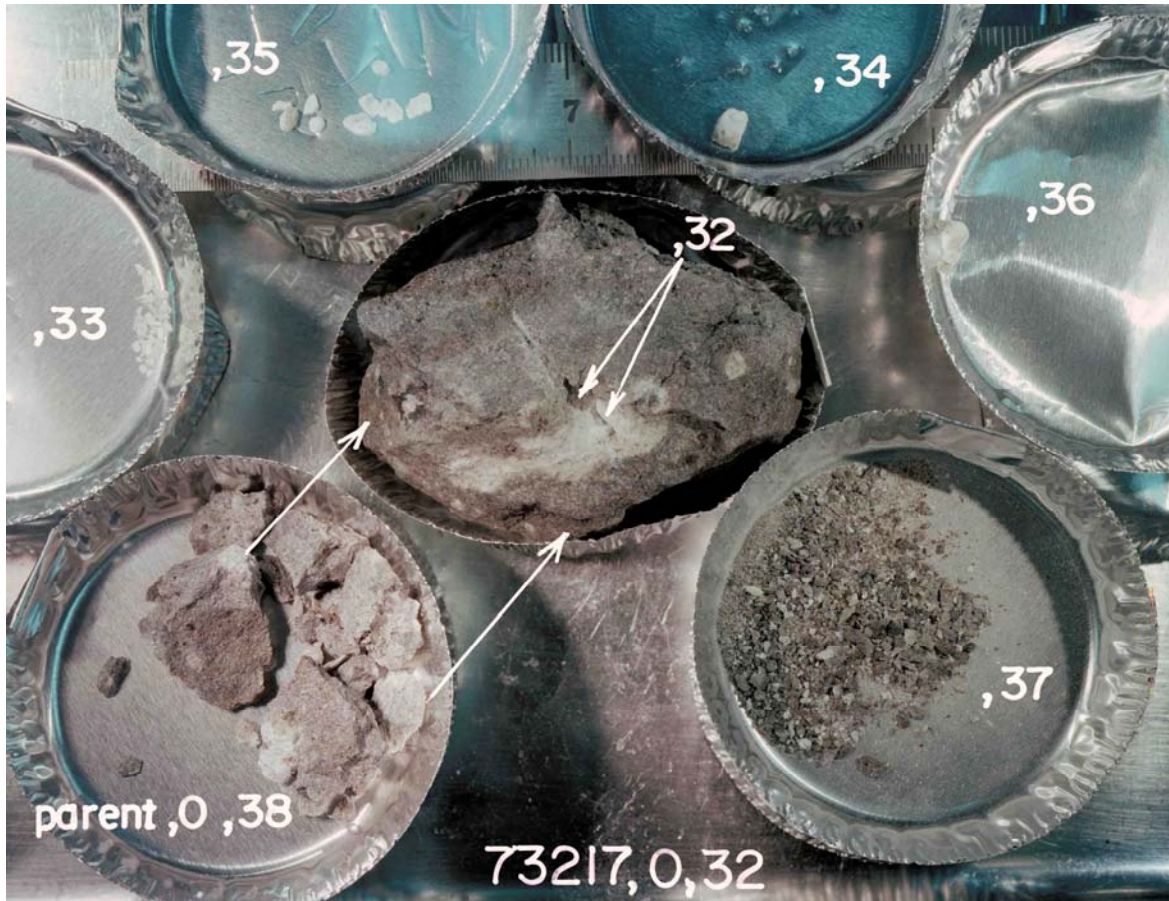


Figure 2: Processing to obtain the prominent white class in 73217. S-81-25234

elsewhere appears to post-date the gabbro. Locally the brown glass is independent of the gabbro, and exists as patches in the groundmass, commonly with coronas, that might be residual melt or reacted clasts. The anorthosite clast is a finely ground, fairly pure cataclasized anorthosite with a broad reaction rim with the matrix.

Crawford (1975 a,b) described the melt groundmass in 73217,15 as grading from a finely granulated aggregate of plagioclase with small amounts of pyroxene to a clear to pale brown glass. She noted an abundance of monomineralic clasts, particularly plagioclase, and proposed that the whole rock was generated by in situ partial melting of the clast population, which in turn had a plutonic, crustal origin. She described and depicted all phases, with microprobe data.. The plagioclase is predominantly anorthitic (near An_{93}), but grains

as sodic as An_{72} are reported. Common glass inclusions appear to be the same composition as the host anorthite. The sodic plagioclases show considerably more melting. Crawford (1975 a, b) distinguished three classes of pyroxene: "plutonic" ortho- and clinopyroxenes with coarse exsolution lamellae; fine-grained pyroxene in coronas; and groundmass melt pyroxene. She diagrammed their compositions (Fig. 4). She interpreted the augite inclusions as products of exsolution during her proposed partial melting of the plutonic rock. The orthopyroxene exsolution suggests equilibration in the original plutonic environment at about 800 degrees centigrade. The brown glass is evolved (e.g. tabulated probe analysis of 81% SiO_2 and 4.4% K_2O) and its difference from bulk melt groundmass, she states, is the best evidence for the partial melting origin. Crawford (1975a) supposes 73217 to be the first convincing case supporting impact triggered partial

melting on the Moon. She concludes that the product of such partial melting is not KREEP basalt.

Ishii et al. (1980, 1981, 1983) made a detailed study of the petrology and thermal history of 73217 from examination of the pyroxene crystallization sequence, pyroxene exsolution, and geothermometry. They used petrographic, microprobe, and x-ray diffraction methods. They too conclude that an early plutonic event was succeeded by a thermal event; however, they disagree with Crawford (1975) that the thermal event was one of in situ partial melting. Ishii et al. (1980, 1981, 1983) describe the breccia (as seen in 72317,26) as a calcic-plagioclase-rich breccia containing abundant angular mineral clasts which are rare lithic

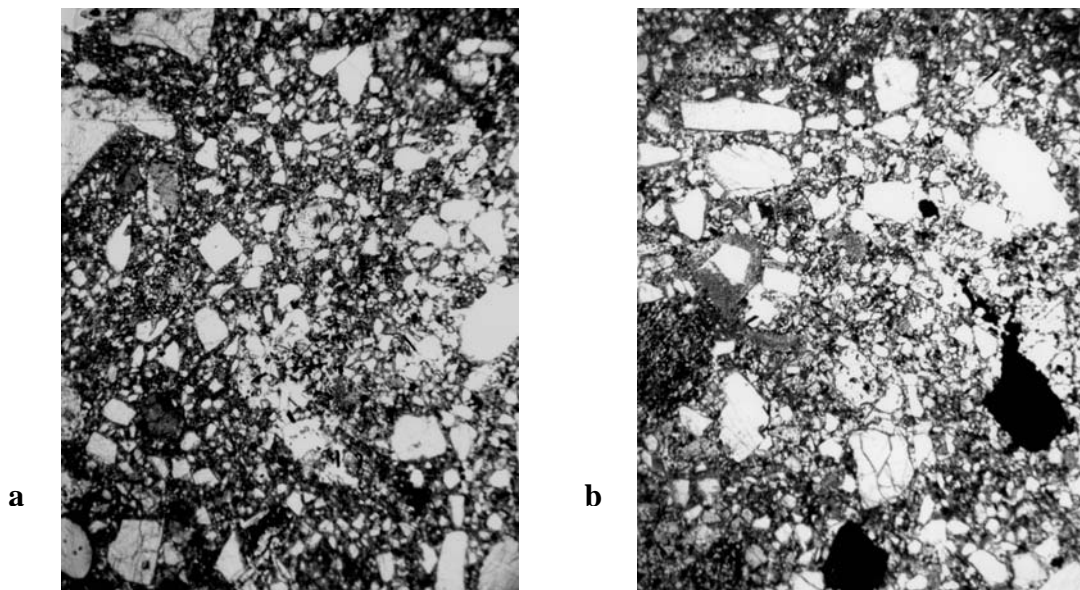


Figure 3: Photomicrographs of 73217,27. Plane transmitted light, fields of view about 2 mm wide. a) general view showing dark fine melt groundmass and abundant angular mineral clasts. b) view showing area dominated by gabbroic lithology with melt groundmass prominent only at top; remainder dominated by crushed gabbro, including plagioclase (white), ilmenite (black), and pyroxenes (pale to gray). Fuzzy phases are small patches of silicic brown glass.

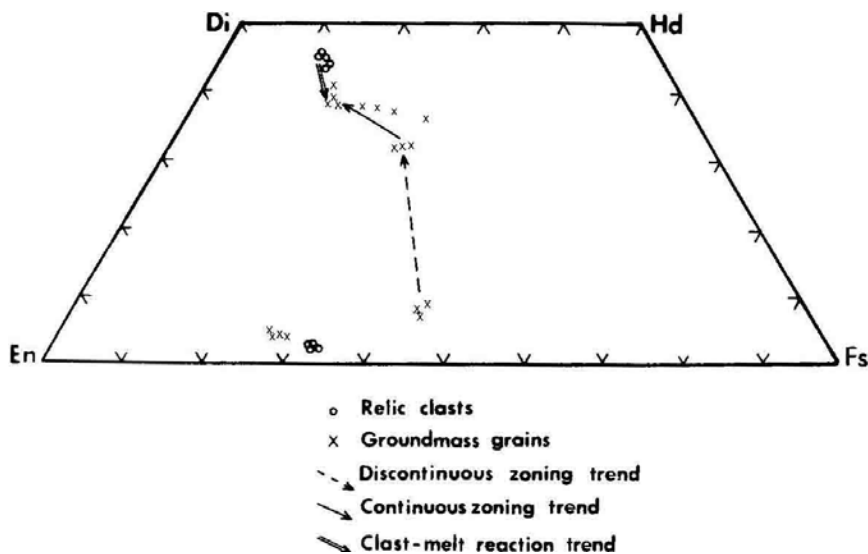


Figure 4: Pyroxene quadrilateral. (Crawford, 1975a).

clasts in a fine-grained, partially glassy matrix. It consists of two domains with a gradational boundary. Domain A contains coarse orthopyroxene clasts, whereas domain B contains coarse pigeonite clasts. The pyroxene trends are analogous to early (A) and late (B) fractionation stages of terrestrial intrusions. Some other small clasts are also described: a gabbroic lithic clast, a troctolitic lithic clast, and dusty augite clasts. The most detailed information on the pyroxenes is presented in Ishii et al. (1983), including tabulated and diagrammed microprobe data (Figs. 5-8), and crystallographic information (Table 1) including precession photographs. Minor element compositions for both high-Ca and low-Ca pyroxenes in both breccia domains vary continuously with Mg' . The optical and X-ray diffraction studies demonstrate a great variety of exsolution textures, but individual pyroxenes show relatively simple exsolution. None of pyroxene, plagioclase, or ilmenite

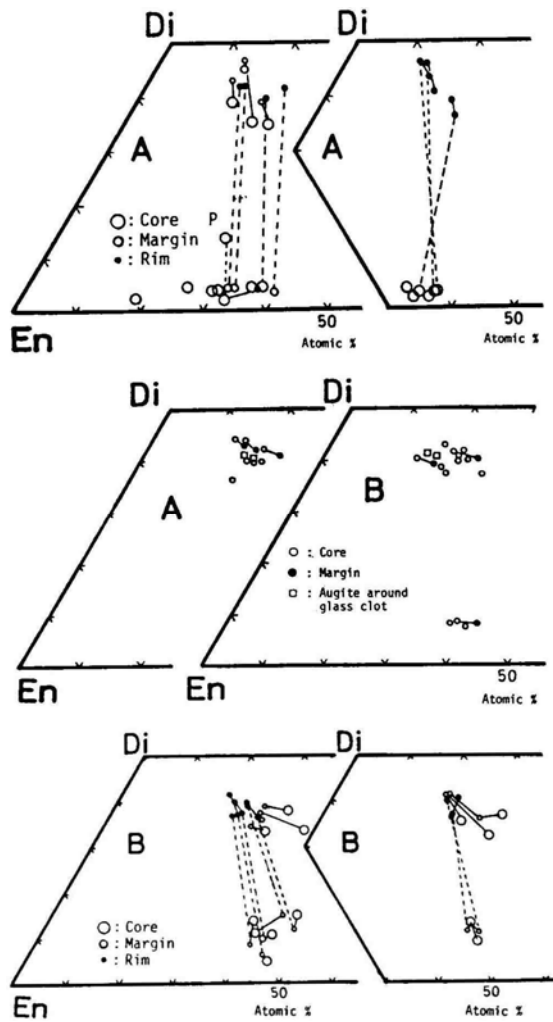


Figure 5: Pyroxene quadrilaterals. (Ishii et al., 1983)

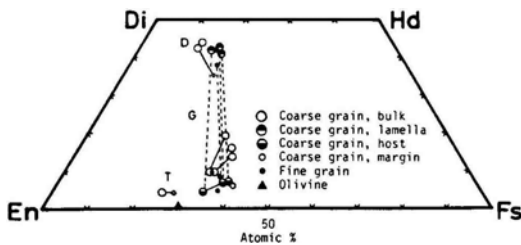


Figure 6: Pyroxene quadrilaterals. (Ishii et al., 1983)

compositions in domains A and B overlap. Ishii et al. (1983) conclude that both domains could be derived from a single pluton, A at the bottom (early, 1100 degrees C or so) and B at the top (later, a few tens of degrees lower temperature). (The troctolitic, etc., lithic clasts are unrelated to this sequence). However, the pyroxene crystallization trend (Figs. 5, 6, 9) is so complicated that at least two or more episodes are required: an early plutonic/hypabyssal event, and a later thermal/annealing event. They propose a first event forming layered bodies, a second event mixing mineral only in the upper part of a pluton (B) and a third event that mixed lower (A) and upper (B). During the latter event temperatures rose to over 1000 degrees C and the rock was partially melted. The precise nature of this latter event is not clarified by Ishii et al. (1983).

Warren et al. (1982 a, b) described the prominent white clast, estimated to weigh about 1.7 g. The boundary between the clast and the groundmass is extremely diffuse. The thin section studied (, 41) includes the boundary area. The central, matrix-free part is almost entirely plagioclase, whereas the diffuse area, presumably contaminated with matrix, contains about 40% pyroxene. The central anorthosite is fine-grained and cataclased. The plagioclase is $An_{90-2-95.4}$ with a mean of $An_{93.3}$. The pyroxene, about $En_{72}Wo_4$, may not even be part of the anorthosite. Warren et al. (1982 a) refer to the clast as "quasi-pristine," i.e., it is likely to be essentially pristine but to have undergone subtle changes.

Compston et al. (1984 a) described and depicted zircon grains and their associated assemblages from 73217, providing zircon microprobe analyses. They describe the host as a clast that has a granitic melt composition that contains seriate mineral clasts of anorthite, augite, hypersthene, ilmenite, and zircon. The zircons are inferred to

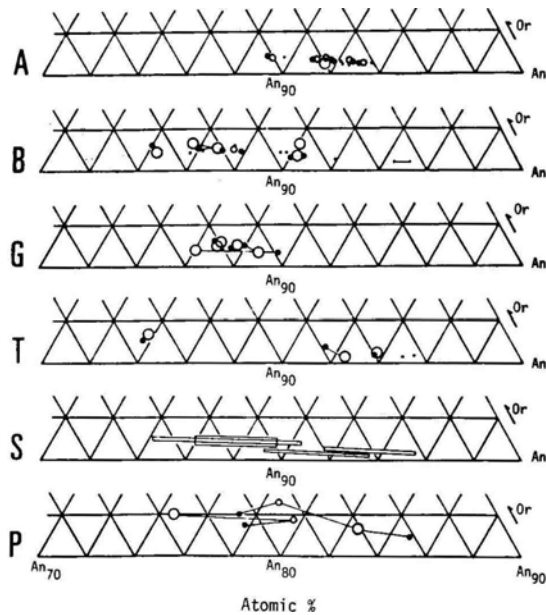


Figure 7: Plagioclase compositions. (Ishii et al., 1983)

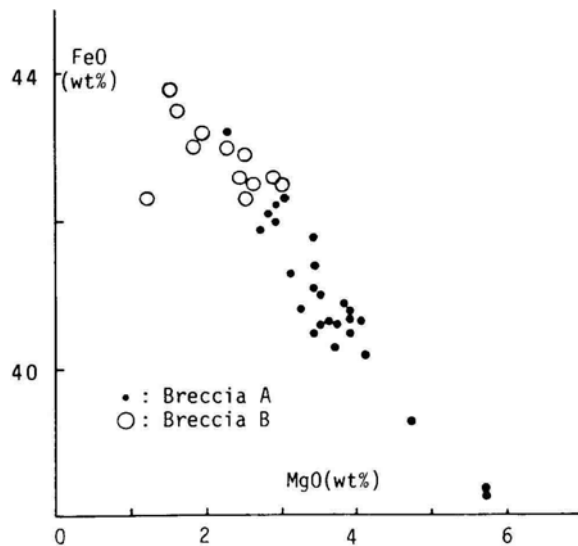


Figure 8: Ilmenite compositions. (Ishii et al., 1983)

be an integral part of the gabbroic igneous assemblage, one zircon being attached to ilmenite. (The zircons were used for ion-microprobe U-Pb isotopic studies). The zircons are anhedral and have evidence of resorption, presumably during the melting of the matrix, and have no overgrowths.

Bersch et al. (1988, 1991) reported precise minor element and major element compositions for some pyroxene grains in 73217, 41; the pyroxene is most likely to derive from clasts in the matrix and not from the anorthosite itself.

CHEMISTRY

The only chemical analyses are two splits of the anorthosite clast, one at least of which is rather impure (Warren et al., 1982 a, b). A single chip was handpicked to separate as much pure white clast as possible from groundmass. The analyses are presented in Table 2. The purer handpicked part appears to be a true anorthosite, as also indicated by the thin section. The pristine nature of the sample is ambiguous on the basis of Au at least, although Ir and Ni are both low. However, the impure separate has no more Au or Ni than the more pure separate. Possibly there has been some diffusion of elements across the boundary with the groundmass. The rare earth elements, while low, have a KREEP pattern (Fig. 10), also indicating some contamination. The sample, on the basis of plagioclase compositions and incompatible element abundances, is not an alkali anorthosite, but is at least close to the established range for ferroan anorthosites.

RADIOGENIC ISOTOPES AND GEOCHRONOLOGY

Four zircons were analyzed for UPb isotopes using high resolution ion microprobe techniques (Compston et al., 1984a, b) (Table 3). The zircons were analyzed in thin sections, and are probably part

Table 1: Crystallographic data for pyroxenes in 73217. (Ishii et al., 1983)

Group‡	Crystal number	Pyroxenes	a(Å)	b(Å)	c(Å)	β (°)	Space group	Analysis* number	Crystall† stage	Remarks
Ia	A 12	Host Augite	9.74	8.91	5.25	106.11	<i>C2/c</i>	19 Aug	Plutonic	50
		(001) Pigeonite	9.74	8.91	5.22	108.00	<i>P2₁/c</i>			
		(100) Orthopyroxene	18.29	8.91	5.24	–	<i>Pbca</i>			
IIa	K 13	Host Orthopyroxene	18.27	8.88	5.21	–	<i>Pbca</i>	23 Pig	Plutonic	20 (volume ratio)
		(100) Augite	9.70	8.88	5.25	105.07	<i>C2/c</i>			
		(100) Orthopyroxene	18.27	8.88	5.21	–	<i>Pbca</i>			
Ib	A 06	Host Augite	9.75	8.93	5.26	105.6	<i>C2/c</i>	05 Aug	A2	–
		(100) Orthopyroxene	18.4	8.9	5.2	–	<i>Pbca</i>			
IIb	B 10	Host Orthopyroxene	18.31	8.88	5.22	–	<i>Pbca</i>	13 Opx	A2	Bushveld type
		(100) Augite	9.73	8.88	5.22	105.40	<i>C2/c</i>			
		(100) Orthopyroxene	18.31	8.88	5.22	–	<i>Pbca</i>			
III	A 11	Host Augite	9.74	8.94	5.26	106.29	<i>C2/c</i>	16 Aug	B1	Chemical zoning
		(001) Pigeonite	9.74	8.94	5.24	108.85	<i>P2₁/c</i>			

of the gabbroic assemblage (one is attached to ilmenite) whose exsolved pyroxenes are so prominent as clasts. The zircons show zoning that is visible microscopically and confirmed by electron- and ion-probe data. All four crystals show little loss of radiogenic Pb, and give U-Pb ages that are within 10% of concordance at $4356 \pm 23, -14$ Ma. (Fig. 11 a, b). This age presumably is that of the igneous event that produced the gabbro, or whatever parent assemblage the zircons reflect. Two of the crystals show evidence of initial radiogenic lead that evolved in a source with $\mu = 2000$. The lower intersect on the concordia diagram is earlier than 1000 Ma, showing that lead loss was not a very recent event. However, the common 3900 Ma lunar event(s) does not show up in this zircon data.

PROCESSING

73217 has never been sawn. In 1973 chips were removed from one end (apparently typical rock) for early allocations including thin sections from potted butt, 11. No samples were taken of the rubbly lithology or of the white clast. 73217 was designated a posterity sample, hence temporarily denied

further processing. Nonetheless, eventually further chipping was carried out (1982) to obtain samples of the prominent white clast (Fig. 2) for chemical and petrographic studies. Further thin sections were cut from a chip (, 10) that had been separated from adjacent , 11 in the original processing.

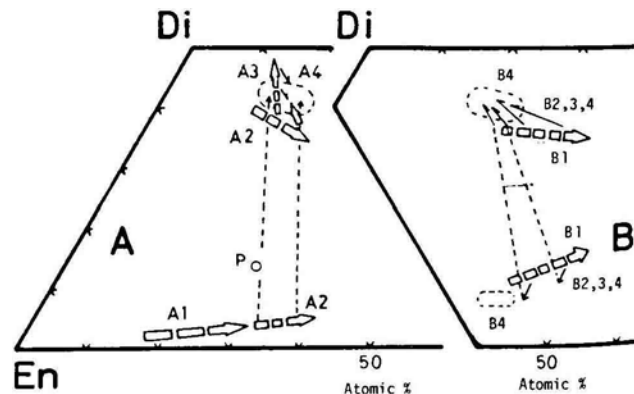


Figure 9: Summary of pyroxene crystallization trends. (Ishii et al., 1983).

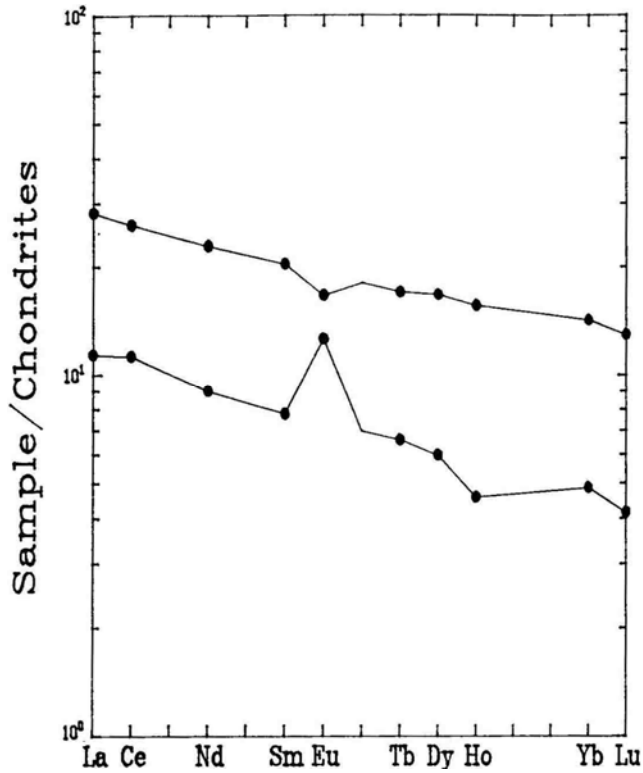


Figure 10: Rare earth elements in pure (lower) and impure (upper) anorthosite samples from prominent white Blast in 73217 (from data of Warren et al., 1982a,b).

Table 2: Chemical analyses of pure (.35 a) and impure (.35b) anorthosite samples from prominent white clast in 73217. (Warren et al., 1982 a, b).

Split	.35a	.35b
wt%		
SiO ₂	44.9	45.8
TiO ₂	.07	.25
Al ₂ O ₃	35.0	31.6
Cr ₂ O ₃	.020	.047
FeO	.77	2.67
MnO	.015	.047
MgO	0.75	2.1021.0
CaO	18.5	16.8
Na ₂ O	0.67	0.73
K ₂ O	0.04	0.115
P ₂ O ₅		
ppm		
Sc	1.91	4.7
V		
Co	5.4	8.9
Ni	6.4	6.8
Rb		7.3
Sr		
Y		
Zr	121	240
Nb		
Hf	1.42	3.4
Ba	190	240
Th	1.10	2.65
U	0.40	0.69
Cs		0.56
Ta	0.16	0.71
Pb		
La	3.75	9.3
Ce	9.9	23.0
Pr		
Nd	5.4	13.7
Sm	1.41	3.69
Eu	0.87	1.15
Gd		
Tb	0.31	0.80
Dy	1.89	5.3
Ho	0.32	1.09
Er		
Tm		
Yb	0.97	2.84
Lu	0.141	0.44
Li		
Be		
B		
C		
N		
S		
F		
Cl		
Br		
Cu		
Zn	0.47	2.2
ppb		
Au	2.27	2.06
Ir	0.04	0.180
I		
At		
Ga	7200	8200
Ge	53	85
As		
Se		
Mo		
Tc		
Ru		
Rh		
Pd		
Ag		
Cd	124	1040
In		
Sn		
Sb		
Te		
W		
Re	<0.20	<0.35
Os		
Pt		
Hg		
Tl		
Bi		

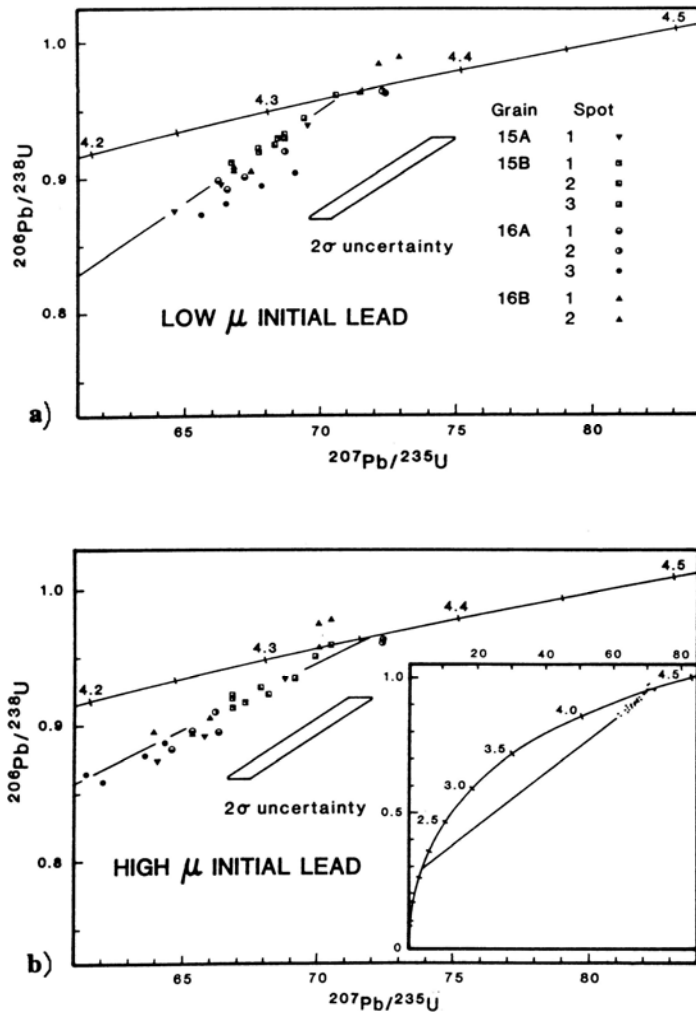


Figure 11: Concordia diagram showing analyses of 73217 zircons, corrected assuming evolution of initial lead in a low u source (a) and a high u source (b) (Compston et al., 1984a). Each point represents the mean of 10 observations of the isotopic composition. In most cases, three such determinations were made at a single spot. Line in a) is reference line for $^{207}\text{Pb}/^{235}\text{U}$ age of grains 15A, 15B, and 16A, 4340 Ma. Age of 16A is higher. Line in b) is best fit with intercepts of 4356 \pm 23, -14 Ma, and 1680 \pm 580 Ma.

Table 3: Summary of ion microprobe data for 73217 zircons. (Compston et al., 1984a).

Spot	U*	Th*	Pb*	$^{232}\text{Th}/^{238}\text{U} \uparrow$	$f\% \downarrow$	$^{208}\text{Pb}_*/^{206}\text{Pb}_*$	$^{208}\text{Pb}_*/^{232}\text{Th}$	$^{207}\text{Pb}_*/^{206}\text{Pb}_*$	$^{206}\text{Pb}_*/^{238}\text{U}$	$^{207}\text{Pb}_*/^{235}\text{U}$
1	300 ± 10	103 ± 4	378 ± 20	0.333 ± 9	0.10 0.32	0.0852 ± 1	0.225 ± 4	0.5370 ± 8 0.5335 ± 6	0.903 ± 18 0.900 ± 18	66.8 ± 1.5 66.2 ± 1.4
1	307 ± 9	215 ± 6	415 ± 12	0.702 ± 3	0.04 0.37	0.1766 ± 6	0.231 ± 3	0.5338 ± 9 0.5294 ± 17	0.918 ± 5 0.917 ± 2	67.6 ± 0.5 67.0 ± 0.2
2	329 ± 8	240 ± 5	456 ± 14	0.728 ± 3	0.03 0.15	0.1818 ± 3	0.234 ± 3	0.5346 ± 7 0.5329 ± 12	0.938 ± 11 0.937 ± 11	69.2 ± 0.7 68.9 ± 0.8
3	396 ± 11	323 ± 8	551 ± 15	0.816 ± 2	0.01 0.00	0.2023 ± 6	0.231 ± 2	0.5345 ± 10 0.5319 ± 31	0.931 ± 7 0.936 ± 8	68.6 ± 0.5 68.6 ± 0.9
1	154 ± 6	136 ± 4	209 ± 8	0.885 ± 11	0.10 0.60	0.222 ± 6	0.224 ± 4	0.5394 ± 25 0.5320 ± 24	0.896 ± 2 0.891 ± 4	66.6 ± 0.3 65.4 ± 0.5
2-1	165	138	229	0.838	0.33	0.2084	0.228	0.5420	0.919	68.7
2-2	174 ± 4	168 ± 8	256 ± 7	0.971 ± 21	1.30	0.2355 ± 5	0.233 ± 1	0.5279	0.910	66.2
2-3					0.50			0.5453 ± 8	0.962 ± 1	72.3 ± 0.1
					0.00			0.5455 ± 5	0.962 ± 1	72.4 ± 0.1
3	141 ± 10	137 ± 10	194 ± 14	0.977 ± 3	0.06 2.10	0.256 ± 3	0.233 ± 3	0.5493 ± 23 0.5225 ± 26	0.888 ± 8 0.872 ± 6	67.2 ± 0.8 62.8 ± 0.7
1	356 ± 49	213 ± 30	469 ± 64	0.597 ± 9	0.05 1.00	0.1547 ± 7	0.235 ± 3	0.5371 ± 22 0.5251 ± 37	0.905 ± 1 0.899 ± 3	67.0 ± 0.2 65.1 ± 0.6
2	373 ± 31	228 ± 18	532 ± 45	0.610 ± 3	0.05 0.80	0.1571 ± 8	0.252 ± 4	0.5353 ± 20 0.5251 ± 33	0.978 ± 8 0.970 ± 7	72.2 ± 0.4 70.2 ± 0.1